TH/P2-2

Sheared flow layer formation in tokamak plasmas with reversed magnetic shear

J. Q. Dong, Y. X. Long, Z. Z. Mou, J. H. Zhang, and J. Q. Li*

Southwestern Institute of Physics, Chengdu, China

* also at Naka Fusion Research Establishment, JAERI, Naka, Ibaraki, Japan

e-mail contact of main author: jiaqi@swip.ac.cn

Abstract Sheared flow layer (SFL) formation due to magnetic energy release through tearing-reconnections in tokamak plasmas is investigated. The characteristics of the SFLs created in the development of double tearing mode, mediated by electron viscosity in configurations with non-monotonic safety factor q profiles and, therefore, two rational flux surfaces of same q value, are analyzed in detail as an example. Quasi-linear simulations demonstrate that the sheared flows induced by the mode have desirable characteristics (lying at the boundaries of the magnetic islands), and sufficient levels required for internal transport barrier (ITB) formation. A possible correlation of the SFLs with experimental observations, that double transport barrier structures are preferentially formed in proximity of the two rational surfaces, is also proffered.

1. Introduction

Internal transport barriers (ITBs) in advanced tokamak (AT) discharges are formed due to turbulent transport suppression by sheared flow layers (SFLs) in accordance with anomalous transport theory. Conditions, especially radial positions, for triggering SFLs and ITB formation, have been intensively investigated in recent years. However, dynamics for SFL and ITB formation is still not well understood yet.

Experimental observations on JT-60U, DIII-D, TFTR, RTP, JET and ASDEX Upgrade show that ITBs are preferentially formed near low order rational flux surfaces, and are often found to associated with presence of MHD activity [1,2]. In addition, SFLs are observed at the boundaries of magnetic islands in LHD experiments [3]. A particularly interesting observation in JET reversed magnetic shear discharges is that two radially separated ITBs simultaneously exist and follow the two $q = 2$ surfaces [4]. The amplitude of the MHD activity (the top part of Figure 8 in Ref. 4) is higher when the double ITB structure exists than it is before the ITB structure is generated. The ITBs are terminated by an $m = 2$ MHD mode which, extending from the inner to the outer foot point location of the two ITBs, has precisely the defining theoretical characteristic of double tearing mode (DTM).

Low order rational flux surfaces are prone to excitation of MHD instabilities. Magnetic energy released in reconnection processes may drive significant plasma flows. Therefore, MHD instabilities are plausible triggering mechanisms for the formation of SFLs and then ITBs. A model for double SFL and ITB structures in tokamak plasmas with reversed magnetic shear (RS) is proposed in this work.

By simulating the nonlinear development of electron viscosity double tearing mode [5], we demonstrate the creation of sizable sheared poloidal flow layers at the boundaries of the magnetic islands. The reduced dissipative 2D MHD equations with electron viscosity included are solved as an initial value problem for a single harmonic of perturbations in a standard sheared slab for simplicity [6].

2. Physical models and basic equations

We consider a plasma slab of length a in the x-direction, with a current in the z- direction, and zero equilibrium flow velocity $\mathbf{V}_0 = 0$ embedded in the standard sheared magnetic field

$$\mathbf{B}_0(x) = B_{0y}(x)\hat{\mathbf{y}} + B_{0z}(x)\hat{\mathbf{z}}, \tag{1}$$

where $B_{0y}(x)$ equals zero at $x = \pm x_s$. The stability of this initial configuration will be examined with respect to two-dimentional, incompressible perturbations. The vector fields are expressible in terms of two scalar potentials : the flux function $\psi(x, y, t)$,

$$\mathbf{B}_\perp = \nabla\psi \times \hat{\mathbf{z}}, \tag{2}$$

and the stream function $\phi(x, y, t)$,

$$\mathbf{V}_\perp = \nabla\phi \times \hat{\mathbf{z}}. \tag{3}$$

With electron viscosity, the Ohm's law becomes

$$\mathbf{E} = \eta\mathbf{j} - \frac{1}{c}\mathbf{V} \times \mathbf{B} - \frac{m_e\mu_e}{n_e e^2}\nabla^2\mathbf{j}. \tag{4}$$

It is straightforward to write the z-component of Eq. (4) as

$$\frac{\partial\psi}{\partial t} = -\mathbf{V}\cdot\nabla\psi + \frac{c^2}{4\pi}\eta\nabla^2\psi - \frac{m_e\mu_e c^2}{4\pi n_e e^2}\nabla^4\psi, \tag{5}$$

after using Eq. (2) and Faraday's law. Here, η is the plasma resistivity, μ_e is the parallel electron viscosity diffusion coefficient, m_e is the electron mass, n_e is the electron density, e and c are, respectively, the electron charge and the speed of light. The z-component of the curl of plasma motion equation may be written as

$$\frac{\partial}{\partial t}(\nabla^2\phi) = -(\mathbf{V}\cdot\nabla)\nabla^2\phi + \frac{1}{4\pi\rho}[\nabla(\nabla^2\psi)\times\nabla\psi]\cdot\hat{\mathbf{z}} + \frac{\mu_i}{\rho}\nabla^4\phi, \tag{6}$$

where ρ is the mass density of the plasma, μ_i is the ion viscosity. Normalizing all lengths to a, time to $\tau_h = a/v_A$, the poloidal Alfvén time of a plasma column of scale width a, and the magnetic field to some standard measure B_0, Eqs. (3), (5) and (6) transform to :

$$\frac{\partial\psi}{\partial t} = \{\phi, \psi\} + \frac{1}{S}\nabla^2\psi - \frac{1}{R}\nabla^4\psi + E', \tag{7}$$

$$\frac{\partial}{\partial t}(\nabla^2\phi) = \{\phi, \nabla^2\phi\} - \{\psi, \nabla^2\psi\} + \frac{1}{R_i}\nabla^4\phi, \tag{8}$$

where $S = \tau_r/\tau_h$ is the magnetic Reynolds number with $\tau_r = 4\pi a^2/c^2\eta$, $R = \tau_v/\tau_h$ is the electron viscosity diffusion Reynolds number, while $\tau_v = 4\pi a^4 n_e e^2/c^2\mu_e m_e = \omega_{pe}^2 a^4/c^2\mu_e, R_i = \tau_{vi}/\tau_h$ is the ion fluid Reynolds number with $\tau_{vi} = \rho a^2/\mu_i$, and

$$\{\phi, \psi\} = \frac{\partial\phi}{\partial x}\frac{\partial\psi}{\partial y} - \frac{\partial\psi}{\partial x}\frac{\partial\phi}{\partial y}$$

is the Poisson bracket. E' is the externally applied electric field to keep the total plasma current constant. It is worthwhile to point out that the first term on the right hand side of Eq. (7) represents so called dynamo effect that may "reorganize" local current density and hence magnetic configuration including safety factor q profile through plasma motion.

The basic idea here is that energy released in magnetic reconnection due to development of tearing modes converts to plasma kinetic energy and thus drives sheared flow layers. Therefore, the necessary condition for the mechanism to work is excitation of tearing instability that may only be induced through dissipative effects such as resistivity or electron viscosity in Ohm's law and then in Eq. (7). On the other hand, ion viscosity may induce momentum transfer to them. However, such transfer is valid only when there exists enough momentum driven by such mechanism as tearing modes in the plasma. Ion viscosity does not induce tearing modes but suppress them. As a result, ion viscosity is included here to provide a saturation mechanism. In accordance with the parity of tearing mode structure, assuming the perturbation potentials

$$\phi = \sum_{m=1}^{\infty} \bar{\phi}_m(x,t)\sin(mky), \tag{9}$$

and

$$\psi = \delta\psi(x,t) + \sum_{n=1}^{\infty} \bar{\psi}_n(x,t)\cos(nky), \tag{10}$$

we obtain the following coupled quasi-linear equations from the first harmonic perturbation,

$$\frac{\partial\delta\psi}{\partial t} = -\frac{k}{2}(\frac{\partial\bar{\phi}_1}{\partial x}\bar{\psi}_1 + \bar{\phi}_1\frac{\partial\bar{\psi}_1}{\partial x}) + \frac{1}{S}(\frac{d^2\psi_0}{dx^2} + \frac{\partial^2\delta\psi}{\partial x^2}) - \frac{1}{R}(\frac{d^4\psi_0}{dx^4} + \frac{\partial^4\delta\psi}{\partial x^4}) + E' \tag{11}$$

$$\frac{\partial\bar{\psi}_1}{\partial t} = -k\bar{\phi}_1(\frac{d\psi_0}{dx} + \frac{\partial\delta\psi}{\partial x}) + \frac{1}{S}(\frac{\partial^2\bar{\psi}_1}{\partial x^2} - k^2\bar{\psi}_1) - \frac{1}{R}(\frac{\partial^4\bar{\psi}_1}{\partial x^4} - 2k^2\frac{\partial^2\bar{\psi}_1}{\partial x^2} + k^4\bar{\psi}_1) \tag{12}$$

$$\frac{\partial}{\partial t}(\frac{\partial^2\bar{\phi}_1}{\partial x^2} - k^2\bar{\phi}_1) = k(\frac{d\psi_0}{dx} + \frac{\partial\delta\psi}{\partial x})(\frac{\partial^2\bar{\psi}_1}{\partial x^2} - k^2\bar{\psi}_1) - k(\frac{d^3\psi_0}{dx^3} + \frac{\partial^3\delta\psi}{\partial x^3})\bar{\psi}_1 + \frac{1}{R_i}[\frac{\partial^2}{\partial x^2}(\frac{\partial^2\bar{\phi}_1}{\partial x^2} - k^2\bar{\phi}_1) - k^2(\frac{\partial^2\bar{\phi}_1}{\partial x^2} - k^2\bar{\phi}_1)]. \tag{13}$$

Such a truncating as employed above may introduce unexpected errors. However, our new results with more harmonics included (not shown in this work and will appear in a separate work soon) indicate that the essential conclusions are not influenced except that the mode reaches saturation due to effects introduced by nonlinear interaction between harmonics.

3. Numerical results

Equations (11-13) are solved as an initial value problem - E' is chosen such that the equilibrium does not dissipate due to resistivity and viscosity.

For the magnetic field, we employ the configuration used in Ref. 6,

$$B_{0y}(x) = 1 - (1 + b_c)\mathrm{sech}(\zeta x), \tag{14}$$

where

$$\zeta x_s = \mathrm{sech}^{-1}[1/(1 + b_c)]. \tag{15}$$

The constant b_c is chosen such that $B'_{0y}(x_s) = \pi/2$. We do not need to specify $B_{0z}(x)$ and $P_0(x)$ since incompressible equations are used. The resistivity and the viscosity are both assumed to be constant. The initial conditions for $\bar{\psi}_1$ and $\bar{\phi}_1$ are the linear eigenfunctions multiplied with a small number and $\delta\psi(t = 0) = 0$.[6] The boundary conditions are $\delta\psi(x) = \partial\delta\psi/\partial x = 0$, and the values provided by the initial conditions such as $\bar{\psi}_1(x) = \partial\bar{\psi}_1/\partial x = 0$, $\bar{\phi}_1(x) = \partial\bar{\phi}_1/\partial x = 0$ for $x = \pm x_w$. The chosen parameters are $k = 0.25$, $R = 10^5$, $S = 9.4 \times 10^5$, $b_c = 0.233509$, $x_w = 4$, $\zeta = 2.68298$ corresponding to two rational surfaces at $x = x_s = \pm 0.25$. The results are checked to be independent of x_w, the grid size and the time-step. Total 501 grid points are used in the simulation domain $[-x_w, +x_w]$ and time-step is 5×10^{-4} for the results given below.

The time evolutions of representative growth rate $\gamma = \partial \ln B_x(x = 0, y = 0)/\partial t$, the total kinetic (the upper curve)

$$E_k = \frac{1}{2}\rho \int (v_x^2 + v_y^2)dxdy = \frac{1}{8\pi}\int [(k\bar{\phi}_1 \cos ky)^2 + (\frac{\partial\bar{\phi}_1}{\partial x}\sin ky)^2]dxdy, \tag{16}$$

and the magnetic energy

$$E_m = \frac{1}{8\pi}\int (B_x^2 + B_y^2)dxdy = \frac{1}{8\pi}\int [(k\bar{\psi}_1 \sin ky)^2 + (\frac{\partial\psi}{\partial x})^2]dxdy, \tag{17}$$

in the simulation domain as functions of time are shown in Figs.1(a), 1(b) and 1(c),

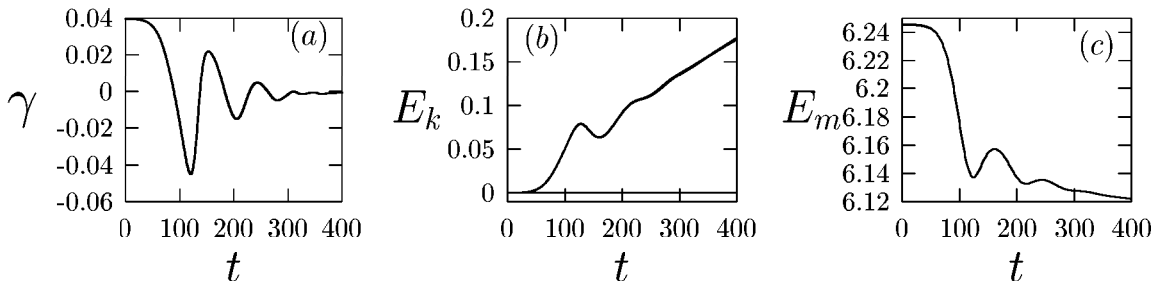

FIG. 1. Time evolutions of representative growth rate (a), total kinetic (the upper curve) (b) and magnetic (c) energies for $R_i = 0$.

respectively. Here, the velocities are measured in units of the poloidal Alfvén velocity in the last expression for E_k, while the magnetic fields are normalized to the poloidal field at plasma boundary. The fact that the magnetic energy released in the reconnection process converts

to kinetic energy is clearly demonstrated. In addition, the energy bounces forth and back between the two states for a couple of times with decaying amplitudes and then goes into a stage when the kinetic and magnetic energy linearly increases and decreases, respectively. Another important fact is that the kinetic energy is almost completely from plasma motion in y-direction. The kinetic energy due to the motion in x-direction is negligibly small as shown by the lower straight line in Fig. 1(b). This means that the driven flow is mainly in poloidal direction of a tokamak, as desired from turbulence suppression theory. Here and afterward, the magnetic fields and the velocities are measured in units of poloidal field and Alfvén velocity at plasma boundary, respectively.

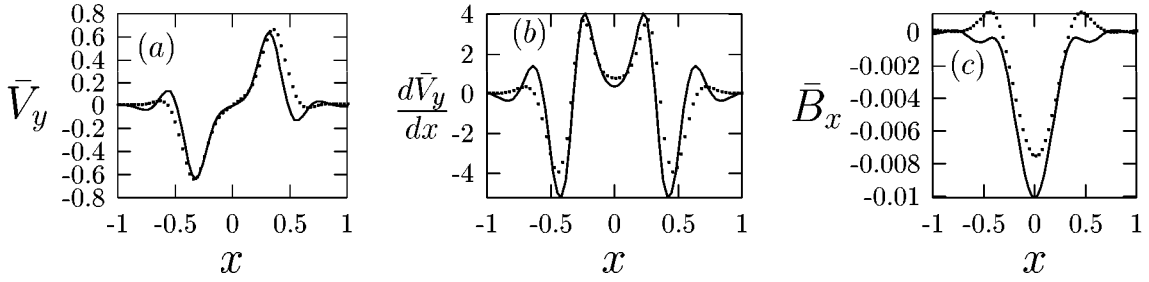

FIG. 2. Profiles of the amplitudes of (a) v_y, (b) $\partial v_y/\partial x$ and (c) B_x at $t = 125$ (the dotted lines) and 170 (the solid lines) for $R_i = 0$.

In Fig. 2, the profiles of the amplitudes of (a) v_y, (b) $\partial v_y/\partial x$, and (c) B_x at $t = 125$ (the dotted lines) and 170 (the solid lines) are presented in the reconnection region which is much smaller than the simulation domain ($-4 \lesssim x \lesssim 4$). Here, x is normalized to a, the scale length in the radial direction. Two very important points emerge: 1) the amplitude of the poloidal velocity v_y reaches the level of poloidal Alfvén velocity, and 2) the flow v_y and flow shear $\partial v_y/\partial x$ are mainly located at the boundaries of the magnetic islands and remain at noticeable levels for $x \gtrsim 0.5$ where B_x is negligibly small.

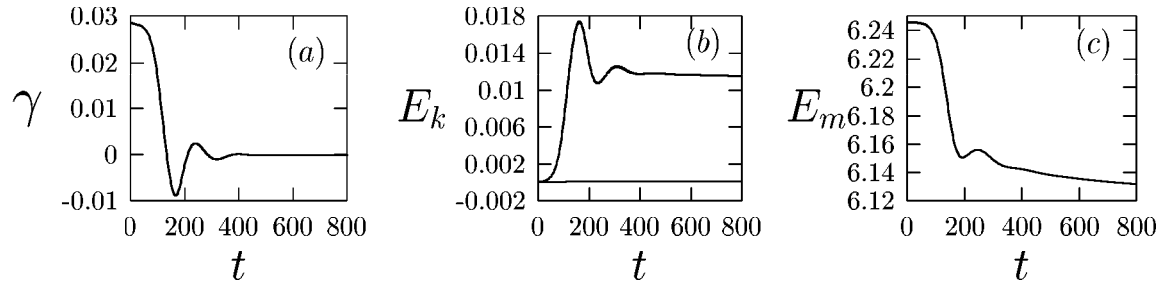

FIG. 3. Time evolutions of representative growth rate (a), total kinetic (the upper curve) (b) and magnetic (c) energies for $R_i = 10^3$.

In Fig. 3, ion viscosity effects on the time evolutions of the representative growth rate (a), the total kinetic (the upper curve) (b) and magnetic (c) energies for $R_i = 10^3$ are presented. The kinetic energy is a constant while the magnetic energy decreases slowly due to ion viscosity after $t = 400$. This is in strong contrast with the results in Fig. 1 where the kinetic energy keeps increasing linearly.

In Fig. 4, the profiles of the amplitudes of (a) v_y, (b) $\partial v_y/\partial x$, and (c) B_x for $R_i = 10^3$ are

presented in the reconnection region. Here the two solid lines are for at $t = 121$, which is the moment when the representative growth rate $\gamma = 0$, (the lines with higher amplitudes) and 800 when the mode is saturated (the lines with lower amplitudes), while the dotted lines are for $t = 200$, 300, 400, 500, 600, 700, respectively. It is clearly shown that he basic characteristics of the profiles do not change from that pointed out above for the case without ion viscosity. However, differences are still visible. Firstly, the profiles of v_y and $\partial v_y/\partial x$ are broader than that when ion viscosity is not taken into account. This is reasonable since the ion viscosity introduces velocity diffusion. Second, the profile of B_x is narrower due to the consumption of the driving energy by the ion viscosity now. Of course, the most notable difference is that the amplitude of the velocity shear is lower than that for $R_i = 0$.

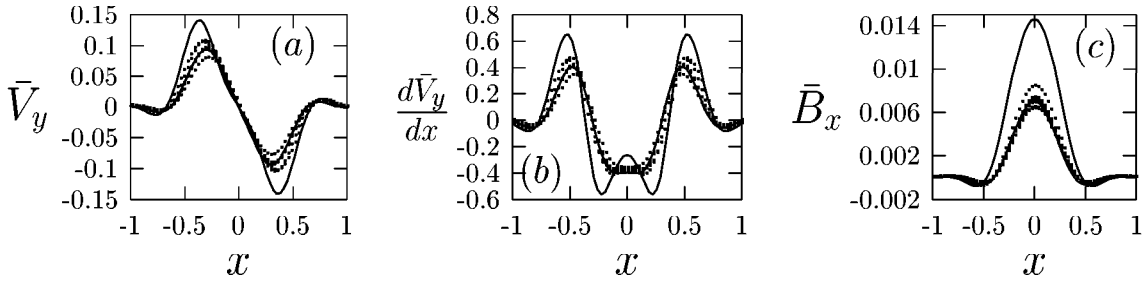

FIG. 4. Profiles of the amplitudes of (*a*) v_y, (*b*) $\partial v_y/\partial x$ and (*c*) B_x for $R_i = 10^3$.

4. Conclusions and discussion

The magnetic energy released in the reconnection process converts to kinetic energy and drive plasma flows in tokamak plasmas. In addition, the kinetic energy is almost completely from plasma motion in y-direction, i.e., the driven flows are mainly in poloidal direction of a tokamak, as required from turbulence suppression theory. Furthermore, the amplitude of the poloidal velocity v_y reaches the level of poloidal Alfvén velocity, and the flow v_y and flow shear $\partial v_y/\partial x$ are mainly located at the boundaries of the magnetic islands and remain at noticeable levels for $x \gtrsim 0.5$ where B_x is negligibly small. The SFLs formed at the boundaries of the magnetic islands on both sides may leads to turbulence suppression and ITB formation in these layers.

In conclusion, the electron viscosity induced double tearing mode is shown to generate localized SFLs in RS plasmas. The nature and magnitude of the flows make the mode a strong candidate for the triggering of ITBs in such tokamak plasmas.

The electron fluid dynamic Reynolds number R, and generated velocity V_y, are estimated as $R \sim 5\times10^7$ and $V_y \propto R^{-1/5} \sim 0.1v_A \sim 0.1v_{ti}$ for $\mu_e \sim 10\text{m}^2/\text{s}$, $\mu_i = 0$ and typical tokamak discharge parameters [7]. The estimated viscous current penetration time, over a plasma of scale length 0.1m, $\tau_v \sim 3.5$s then, does not contradict the experimental evidence [1].

It has to be pointed out that the sheared flows discussed here are periodic in the poloidal direction not like the zonal flows that are constant. However, the suppression effects of sheared flows are independent of the sign of the flows according the turbulence theory. Therefore, the periodic property of the flows does not prohibit them from turbulence suppression. In addition, the shearing rates of the sheared flows created by the tearing modes have not

to be higher than the maximum growth rate of the turbulence driving instability although the values calculated are high enough. This is because that there may be other sheared flow creation mechanisms working together with that discussed in this work. Actually, as experiments have demonstrated that plasma confinements are improved when there are MHD activities with appropriate amplitudes while the confinements are degraded even destroyed when the MHD activities are too strong or violent [4]. This means that MHD activities have to be controlled at appropriate level in order to let it benefit plasma confinement through triggering ITB formation.

This work is supported by the National Natural Science Foundation of China, Grant No. 10135020.

References

[1] R. C. Wolf, Plasma Phys. Control. Fusion **45**, R1 (2003), and the References therein.
[2] J. Connor, T. Fukuyama, X. Garbet *it al.*, Nucl. Fusion **44** R1 (2004).
[3] K. Ida *et al.*, Phys. Rev. Lett. **88**, 015002 (2002).
[4] E. Joffrin *et al.*, Plasma Phys. Control. Fusion **44**, 1739 (2002).
[5] P. K. Kaw *et al.*, Phys. Rev. Lett. **43**, 1398 (1979).
[6] J. Q. Dong *et al.*, Phys. Plasmas **10**, 3151 (2003).
[7] J. Q. Dong *et al.*, accepted for publication in Phys. Plasmas **11**, (2004).